Published in: "Gallium Nitride Materials and Devices VI", Eds. J.-I. Chyi, Y. Nanishi, H. Morkoç, J. Piprek, and E. Yoon, Proc. of SPIE, vol. 7939 (2011) 79391C / **DOI** 10.1117/12.872842

Modeling of III-nitride Light-Emitting Diodes: Progress, Problems, and Perspectives

Sergey Yu. Karpov*

STR Group – Soft-Impact, Ltd., P.O.Box 83, 27 Engels av., St.Petersburg, 194156 Russia

Keywords III-nitride semiconductors, LEDs, simulation, internal quantum efficiency, current spreading, light extraction efficiency, light conversion

Recent progress in III-nitride LED modeling is reviewed with the focus on physical models that provide a better understanding of such hot issues, as factors limiting the internal quantum efficiency of light emission and high-current efficiency droop, polarization doping in graded-composition III-nitride alloys and its utilization in LEDs, current crowding in LED dice and its impact on the light extraction efficiency, and optimal light conversion in white LED lamps. Specific features of III-nitride materials, their impact on the LED operation, and models accounting for these features are considered. Insufficient understanding of transport mechanisms of non-equilibrium electrons and holes and their localization in InGaN inhomogeneous active regions are discussed along with other still unsolved problems. Influence of technological factors on LED heterostructures and their operation is argued in the context of further model developments.

Preprint 2011

1 Introduction Demonstration of high-brightness III-nitride blue light-emitting diodes [1,2] (LEDs) in 1994-1995 kicked out emerging development of production technology for visible and white LEDs based on phosphor-conversion. To date, such LEDs have occupied the major sector on the market of optoelectronic devices. This technological breakthrough was primarily made due to ever improving quality of III-nitride epitaxial materials and increasing efficiency of light extraction (LEE) out of LED dice, from ~25-30% at the earlier stage of development [3] up to ~75-80% in 2003-2006 years [4,5]. Surprisingly, the progress in the fabrication technology left far behind understanding of fundamental physical properties of III-nitride semiconductors and devices. It was recognized rather soon that localized states formed in InGaN quantum wells (QWs) due to composition fluctuations had a great positive impact on internal quantum efficiency (IQE) of LEDs, suppressing the nonradiative carrier recombination at threading dislocations (TDs) [6]. However, considerable spontaneous and strong piezoelectric polarization in nitride compounds was discovered only in 1997-2001 [7-9]. The bandgap of InN was reliably established in 2002 [10]. And, the importance of Auger recombination in wide-bandgap III-nitride compounds and alloys has been just recently started to discuss [11,12]. Many of the above materials properties were unique and had no analogs among conventional III-V compounds. Some of them, like polarization ones or high threading dislocation density (TDD) inherent in epitaxial heterostructures, made the operation of III-nitride devices quite peculiar, which required to largely reconsider conventional approaches to LED design.

At the moment, the LED industry has entered on the way of gradual improvement of LED characteristics based on detailed optimization of every particular unit of the LED design. On the one hand, this necessitates a deeper insight into fundamentals underlying the LED operation and specific features of III-nitride materials making them so different from conventional III-V compounds. On the other hand, the current trends in development of growth equipment for LED mass production result in ever increasing cost of their experimental optimization. In such a situation, the role of modeling and simulation becomes especially important, as they may save considerably money, man power, and time for optimization of available and development of new types of LED. The only question is, however, whether the modern theory is capable of (i) predicting the main directions of further improvement of the LED performance and (ii) estimating, at least roughly, the value of suggested improvements.

* Corresponding author: E-mail sergey.karpov@str-soft.com, Phone: +7 812 554 4570, Fax: +7 812 26 6194, Web site: http://www.str-soft.com

Published in: "Gallium Nitride Materials and Devices VI", Eds. J.-I. Chyi, Y. Nanishi, H. Morkoç, J. Piprek, and E. Yoon, Proc. of SPIE, vol. 7939 (2011) 79391C / **DOI** 10.1117/12.872842

This paper is aimed at addressing the latter key question. Here, the recent progress in modeling III-nitride LEDs will be briefly reviewed and still existing problems are highlighted. Finally, possible directions of further model developments are discussed.

2 Advances in modeling III-nitride LEDs Extensive modeling research of III-nitride LEDs started in about 2004 [13,14], though first simulations of the laser diodes were made some earlier [15]. According to the fabrication levels existing in the LED industry, one can distinguish three levels of simulation models: heterostructure, chip, and LED lamp ones. The carrier transport and injection in the active region, carrier losses, and radiative recombination, are the primary subjects of study on the first of the levels aimed at maximizing IQE of an LED structure. Optimization of current spreading in LED dice, minimization of the diode series resistance, and increasing of LEE are the main goals of modeling on the chip level. And, improving the efficacy, optimization of light conversion, and providing an appropriate heat sink and stability of color characteristics of a white-light LED lamp are the major aims of simulations on the third level. Key physical models and approaches necessary for effective III-nitride LED simulations are discussed below.

2.1 Factor affecting IQE and its high-current droop Because of lacking native GaN or AlN substrates, III-nitride heterostructures are conventionally grown on commercially available sapphire or silicon carbide wafers being highly lattice-mismatched with nitride semiconductors. As a result, a huge amount of TDs normally appears in the epitaxial layers. Typical TDD in the epilayers grown by Metalorganic Vapor-Phase Epitaxy (MOVPE) was ~10^9-10^{10} cm^{-2} in 1990s and has been reduced to ~4-5×10^8 cm^{-2} to date. Being nonradiative recombination centers in III-nitride semiconductors, TDs lower IQE of radiative recombination, control the electron, τ_n , and hole, τ_p , life times (Fig.1a), and determine the carrier diffusion lengths, $L_{n,p} = (D_{n,p}\tau_{n,p})^{1/2}$ where D_n and D_p are the carrier diffusion coefficients. The diffusion coefficients are related to the electron and hole mobilities, μ_n and μ_p , by the Einstein equation: $D_{n,p} = (kT/q)\mu_{n,p}$ where k is the Boltzmann constant and T is temperature. The model of dislocation-mediated carrier life times suggested in Ref. [16] provides a pretty good agreement between the theoretical and measured electron and hole diffusion lengths in p-GaN and n-GaN, respectively (Fig.1c). The model also predicts the carrier life times to be temperature dependent (Fig.1b) and to increase with lowering the carrier mobility. The latter just explains the difference between the electron and hole life times seen in Fig.1a,b.

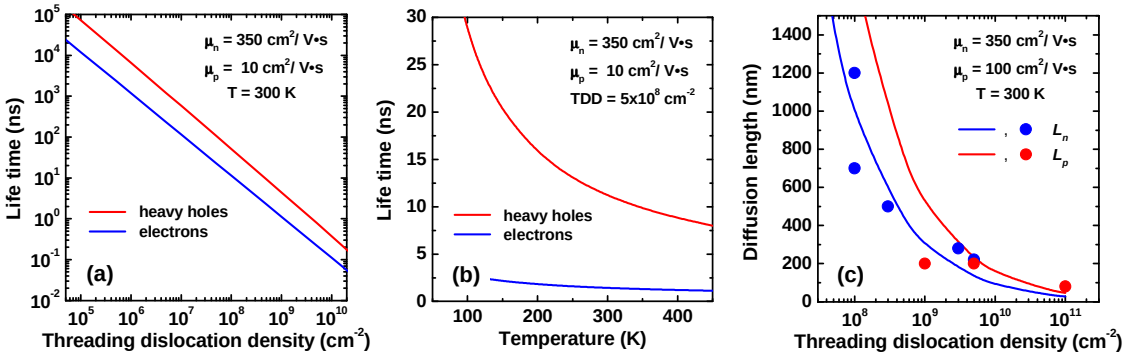

Fig.1 Electron and hole life times as a function of TDD (a) and their temperature dependence (b) calculated by the model of Ref. [16]. Comparison of experimental (circles) and theoretical (lines) electron and hole diffusion lengths, in moderately doped n-GaN and lightly doped p-GaN (c). The data on the diffusion lengths are compiled in Ref. [16].

In addition to the nonradiative electron and hole recombination at TDs, one more origin of the carrier losses is Auger recombination intensifying at high carrier concentrations in the LED active regions. The importance of Auger recombination in III-nitride semiconductors has been in doubt for a long time because of the well known trend of the Auger recombination coefficient to decrease with the materials bandgap in most of conventional III-V compounds (grey line in Fig.2a). However, detailed examination of experimental data has revealed the existence of different trend for the Auger coefficients of AlGaAs, GaP and some group-IV semiconductors [11] (black line in Fig.2a). It looks like there is a universal

Published in: "Gallium Nitride Materials and Devices VI", Eds. J.-I. Chyi, Y. Nanishi, H. Morkoç, J. Piprek, and E. Yoon, Proc. of SPIE, vol. 7939 (2011) 79391C / **DOI** 10.1117/12.872842

lower limit for the Auger recombination coefficient of these materials, ~5×10^{-31}-2×10^{-30} cm^6/s, irrespective of their bandgap. Experimental data obtained by photoluminescence and other techniques, reported in Ref. [12] and following publications, have shown InGaN to obey rather the latter trend (stars in Fig.2a). The Auger coefficients measured for InGaN are found to weakly depend on the alloy composition and to range between ~10^{31} and ~10^{30} cm^6/s. To obtain such a value theoretically, one should consider the Auger processes involving not only the principal conduction and valence bands but also upper and lower ones [18], i.e. to make full-band analysis of all possible recombination channels.

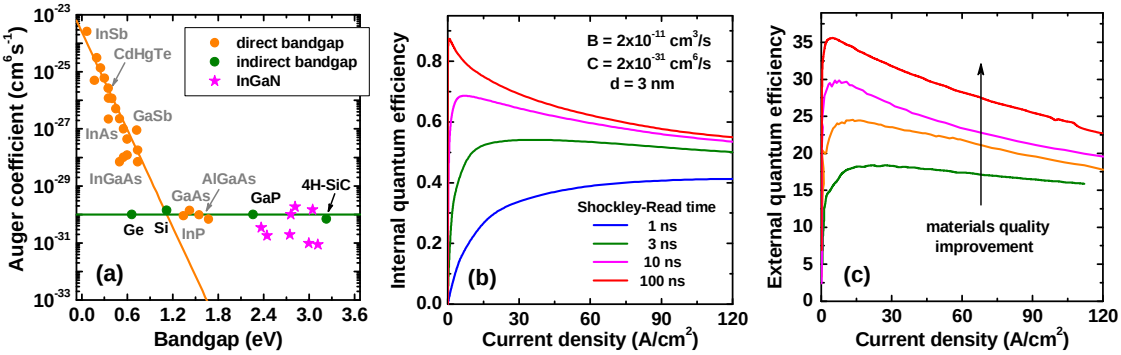

Fig.2 Experimental data on the Auger recombination coefficient (symbols) *versus* energy gap in group-IV and III-V semiconductors (a): lines are plotted for eyes to demonstrate different trends for direct- and indirect-bandgap materials [11], data for InGaN are borrowed from Ref. [17]. IQE of 3 nm InGaN SQW as a function of current density calculated by ABC-model for various nonradiative carrier life times (b). LED efficiency as a function of operation current measured in the diodes with different materials quality [19] (c).

Detailed understanding of recombination mechanisms is quite critical in light of continuing discussion on the origin of high-current IQE droop that occurs practically in all visible III-nitride LEDs at the current densities of ~0.3-30 A/cm^2 irrespective of particular structure design, emission wavelength, and crystal orientation. In other words, the efficiency droop seems to be a universal phenomenon which invokes a universal mechanism to be explained. It is Auger recombination that may be such a universal mechanism capable of explaining the efficiency droop. Assuming the electron, n , and hole, p , concentrations in the LED active region to be nearly equal to each other and neglecting the carrier leakage from the active layer, one can estimate IQE and respective current density j by using the simple so-called ABC-model:

$$j = qd\,(An + Bn^2 + Cn^3)\ ,\quad \mathrm{IQE} = Bn/(A + Bn + Cn^2)\ ,\quad A = 1/\tau_{SR} \tag{1}$$

where q is the electron charge d is the active region width, τ_{SR} is the Shockley-Read nonradiative carrier life time, and B and C are the radiative recombination constant and Auger recombination coefficients, respectively. Fig.2b plots IQE as a function of current density calculated by the ABC-model for various values of τ_{SR} . The model predicts (i) considerable IQE droop in the case of high-quality materials (long τ_{SR}) caused by intensification of Auger recombination at high current densities and (ii) strong shift of the IQE maximum to lower current densities, while increasing the carrier life time. These predictions correlate well with available observations (see, for instance, Fig.2c). It is interesting that no noticeable efficiency droop may be clearly observed in the case of low-quality LED structures (see lower curves in Fig.2b and Fig.2c). So, the droop should be always considered in context with the absolute value of the LED efficiency being the measure of materials quality.

Auger recombination is not, however, the only mechanism controlling IQE of III-nitride LEDs. Recently, a dramatic IQE rise in the low-current density range has been observed in green SQW LEDs at temperatures as low, as 4-250 K, which could not be associated with any simple recombination model [20]. To explain this observation, the idea of carrier localization in InGaN QW due to its composition/thickness fluctuations can be invoked [21]. It is assumed the ensemble of free and localized electrons/holes to have a smooth density of states described by the sigmoid function

$$g(E) = (N_{2D}/kT)\cdot\left[1 + \exp(E - E_0/U)\right]^{-1} \tag{2}$$

Published in: "Gallium Nitride Materials and Devices VI", Eds. J.-I. Chyi, Y. Nanishi, H. Morkoç, J. Piprek, and E. Yoon, Proc. of SPIE, vol. 7939 (2011) 79391C / **DOI** 10.1117/12.872842

where $N_{2D}= (mkT/\pi\hbar^2)$ is the 2D effective carrier density of states, m is the electron/hole effective mass, $\hbar$ is the Plank constant, E is the carrier energy, E_0 is the energy of the ground electron or hole state, and U is the specific energy corresponding to the extension of density of states tails in the bandgap. The states with $E < E_0$ are considered as localized ones, while those with $E > E_0$ are delocalized, belonging to either conduction or valence band. At $U \to 0$, $g(E)$ becomes a conventional step-like function typical for 2D density of states.

Since localized carriers cannot move laterally in the QW, they do not participate in nonradiative recombination at TDs. This can be accounted for in the ABC-model by using the constant $A=f_n f_p/(f_n\tau_p+f_p\tau_n)$ in Eqs.(1) [21], where f_n and f_p are the fractions of delocalized electrons and holes dependent on the quasi-Fermi level position relative to the energy level E_0 and the strength of fluctuations accounted for by the parameters U (Fig.3a). Since the fractions f_n and f_p can be much less than unity at $U \geq kT$, the fluctuations are capable of considerable suppressing the dislocation-mediated nonradiative recombination in InGaN with regard to materials having no such fluctuations, like GaN (see Fig.3b). Just the availability of fluctuations has determined the advantage of using InGaN as the basic materials for active regions of III-nitride LEDs.

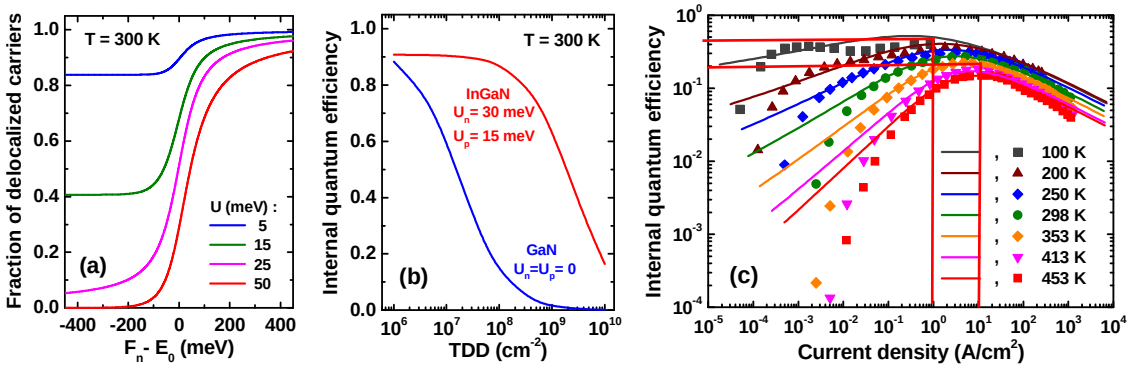

Fig.3 Fraction of delocalized states in a QW as a function of the Fermi level position (a). Calculated IQE of InGaN and GaN as a function of TDD accounting for the effect of localized states in InGaN; here the equal electron and hole concentration of 10^{17} cm^{-3} is assumed (b). IQE of a green SQW LED in a wide range of current density and temperature variation: comparison of experimental data [20] (symbols) and theoretical predictions [21] (lines) (c).

Accounting for the localized states effect on the rate of nonradiative carrier recombination at TDs in combination with the IQE droop caused by Auger recombination enabled a clear interpretation of the data reported in Ref. [20] (see Fig.3c). At low current densities, IQE is largely affected by filling the localized states, which strongly depends on temperature. In particular, almost total carrier localization at a low, less than 200 K, temperature results in remarkable improvement of the low-current LED efficiency. In contrast, high-current IQE is rather controlled by Auger recombination weakly affected by temperature, producing a nearly universal IQE droop in this current density range.

The above approach provides a more or less completed recombination model for the active regions of III-nitride LEDs capable of describing rather complex IQE behaviour observed in experiments, including the high-current efficiency droop. An alternative widely discussed explanation for the droop considers electron leakage in the *p*-region of LEDs. This model is discussed in detail in Ref. [17].

2.2 Polarity effects and polarization doping Polarization charges induced at the interfaces of III-nitride device heterostructures affect dramatically their operation. In particular, separation of electron and hole wave functions in LED QW active regions produced by the charges is commonly considered as a negative effect, resulting in a lower light emission probability. On the other hand, polarization charges provide remarkable impurity-less doping in heterojunction field-effect transistors (FETs). The latter positive effect is undervalued by LED developers and, hence, its potential is not yet utilized in full measure.

It has been recognized already in earlier studies that N-polar LED structure provides a strong natural carrier confinement in the active region, including SQW, suppressing any electron and hole leakage [22]. This fact can be clearly illustrated by Fig.4 comparing the electron and hole current densities in 405 nm laser diode structures on Ga-polar and N-polar substrates. The Ga-polar structure exhibits strong electron

Published in: "Gallium Nitride Materials and Devices VI", Eds. J.-I. Chyi, Y. Nanishi, H. Morkoç, J. Piprek, and E. Yoon, Proc. of SPIE, vol. 7939 (2011) 79391C / **DOI** 10.1117/12.872842

leakage (Fig.4a), which is completely suppressed in the N-polar structure (Fig.4b). As a result, the N-polar structure shows exceptionally high injection efficiency (IE) not degrading even at the current densities as high, as ~10-20 kA/cm^2 (Fig.4c). A similar but slightly weaker effect is also predicted for non-polar [22] and semipolar structures. The reason for such a drastic difference between the Ga-polar and N-polar structures is the polarization charge induced at the spacer/electron blocking layer (EBL) interface. Being positive in the case of Ga-polarity, the polarization charge moves down the potential barrier formed in the EBL. In contrast, the negative charge formed in the case of N-polarity provides the barrier moving up. As a result, EBL works much better in the N-polar laser diode structure compared to the Ga-polar one.

An interesting and important opportunity for designing LED structures can be opened by distributed polarization doping (DPD) in graded-composition III-nitride alloys. Experimentally, DPD has been used for the first time to form high electron concentration in bulk-AlGaN/GaN FETs with graded-composition AlGaN cap layer [23]. For LEDs, much more tempting is, however, utilizing DPD to form in the structure regions with a *p*-type conductivity. In particular, it has been shown theoretical that a graded-composition EBL with *p*-type DPD is capable of considerable suppressing the electron leakage in a UV laser diode [24].

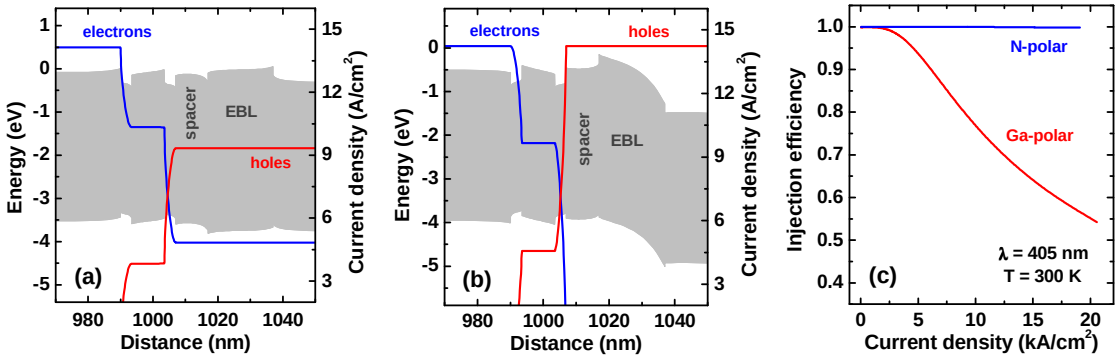

Fig.4 Room-temperature band diagrams and partial electron and hole current densities in 405 nm laser diode structures on a Ga-polar (a) and N-polar (b) GaN substrates, simulated for the current density of 14 kA/cm^2. Injection efficiency (the fraction of current recombined in the active regions) of the structures as a function of current density (c).

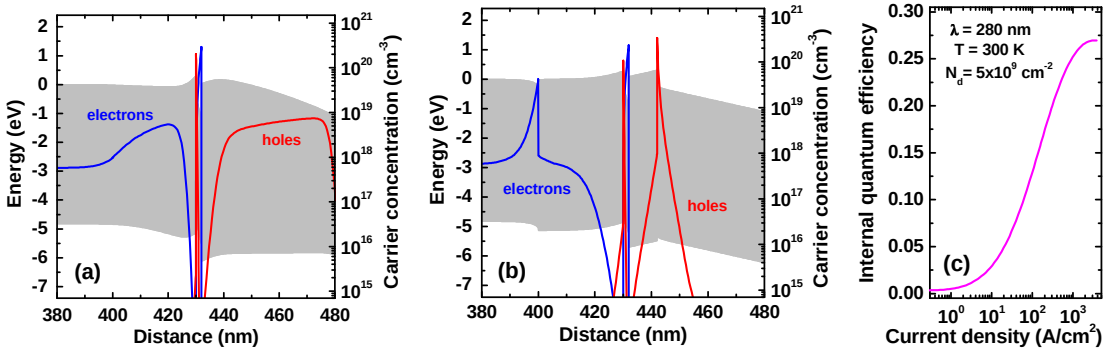

Fig.5 Room-temperature band diagrams and distributions of carrier concentrations in a deep-UV LEDs with graded- (a) and constant-composition (b) designs computed for the current density of 85 A/cm^2. Predicted IQE *versus* current density of the graded-composition LED corresponding to TDD of 5×10^9 cm^{-2} (c).

The feasibility of *p*-type DPD has been recently demonstrated experimentally by growing N-polar graded-composition *p*-$Al_xGa_{1-x}N$ with x linearly increasing from zero to 0.16 or 0.30 at the top of the alloy [25]. A temperature-independent hole concentration of ~0.7-1.5×10^{18} cm^{-3} and a room-temperature Hall mobility of ~5-15 cm^2/V·s were obtained in these graded-composition layers. The absence of temperature dependence of the hole concentration is due to the fact that DPD does not involve any acceptor impurities having a certain activation energy. Therefore, holes cannot be frozen in the DPD compounds

Published in: "Gallium Nitride Materials and Devices VI", Eds. J.-I. Chyi, Y. Nanishi, H. Morkoç, J. Piprek, and E. Yoon, Proc. of SPIE, vol. 7939 (2011) 79391C / **DOI** 10.1117/12.872842

at low temperatures, in contrast to materials doped with impurities. These and other advantages of *p*-type DPD are still waiting for their wide utilization in LED and laser diode heterostructures.

2.3 Current crowding in LED dice and its effect on LED performance Current crowding in LED dice, i.e. current localization near the edges of metallic electrodes, is the phenomenon historically originated from utilization of insulating sapphire substrates for growth of LED structures. This required using the planar chip designs with on-one-side *p*- and *n*-electrode configurations. The current crowding is negligible in vertical LED dice fabricated on thick conductive SiC substrates. However, recent trends in the LED design based on a substrate separation after growing heterostructure, using solid highly reflective *p*-electrode, and deposition of a small-area *n*-electrode on the back side of the LED structure call a new interest to analysis of the current crowding in such dice.

Earlier simulations have shown the current crowding to be of essentially 3D character [13] and to depend on temperature via thermal activation of donors and acceptors in the contact layers [26,27]. More recent studies have found that analysis of the current spreading in LED dice should be coupled with simulations of light extraction in order to understand better particular mechanisms of the current crowding impact on the LED performance [28]. These mechanisms are considered below in more detail.

Because of current crowding, the LED series resistance R_s is quite sensitive to electrode geometry and properties of a thick *n*-contact layer normally used in almost all III-nitride LEDs. Results of full 3D modeling are found to agree well with a simple estimate for the series resistance: $R_s \approx \rho_n L_{sp}/(P d_n)$ where ρ_n and d_n are the specific resistance and thickness of the *n*-contact layer, P is the total perimeter of the *n*-electrode neighbouring upon the active region, and L_{sp} is the current spreading length that can be found from coupled current spreading/thermal simulations. The latter parameter is mainly determined by nonlinear characteristics of the *p*-*n* junction and, to a lesser extent, by other factors, including resistances of the *n*- and *p*-contact layers. The above estimate leads to an amazing conclusion: the stronger the current crowding the smaller is L_{sp} and, hence, the lower is the LED series resistance. So, the crowding cannot be considered as a negative factor in terms of the LED series resistance.

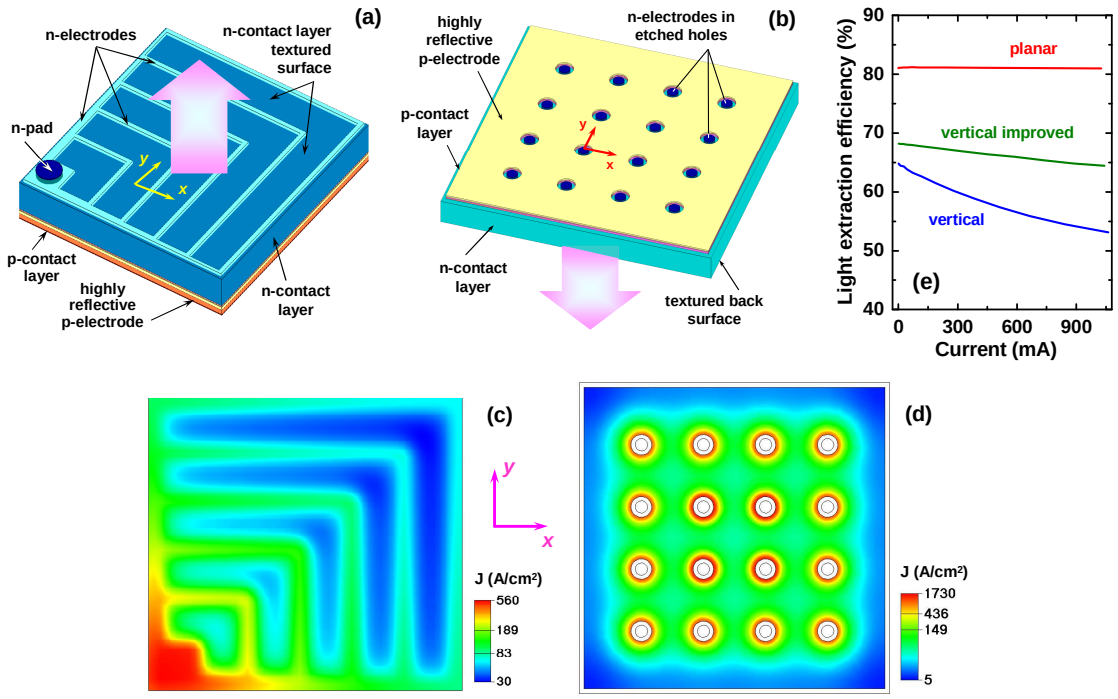

Fig.6 Advanced vertical (a) and planar (b) LED dice with separated substrates and current density distributions in the active regions of the dice computed with SimuLED package [29] (c,d), corresponding to the mean current density of 96 A/cm^2. Comparison of LEE from the vertical, improved vertical, and planar dice (e). Decrease of LEE with current in the case of vertical dice is caused by current localization under and near the poorly reflective metallic *n*-electrodes [28].

Published in: "Gallium Nitride Materials and Devices VI", Eds. J.-I. Chyi, Y. Nanishi, H. Morkoç, J. Piprek, and E. Yoon, Proc. of SPIE, vol. 7939 (2011) 79391C / **DOI** 10.1117/12.872842

On the other hand, high current density produced by current crowding results in a lower IQE in the regions of current localization because of enhanced Auger recombination (see Sec.2.1), which negatively affects the LED performance. Additionally, in some vertical LED dice with separated substrates and *n*-electrodes deposited on the back side of the structure (Fig.6a) the current tends to localize under the electrodes and, especially, under *n*-pad (Fig.6c). Since the reflectivity of the metallic electrodes may be insufficiently high, such a current localization results in the losses of the emitted light via its incomplete reflection from the metal. The effect becomes ever stronger with the LED operation current, making the LEE from the dice to depend on the current (Fig.6e). Actually, this is one more mechanism contributing to the overall droop of the LED efficiency originated from the current crowding [28]. This effect can be suppressed by inserting a thin insulating film under the *n*-pad and using narrower strip electrodes with reduced spacing (improved die design suggested in Ref. [28]). Complete removal of the *n*-electrodes from the back surface of LED structure, as it was made, for example, in the planar (with on-one-side electrode geometry) LED die shown in Fig.6b, enables avoiding the LEE dependence on the operation current (Fig.6e). In the latter case, however, the current crowding is more pronounced because of a small *n*-electrode perimeter (Fig.6d), which may give rise to the long-term device degradation.

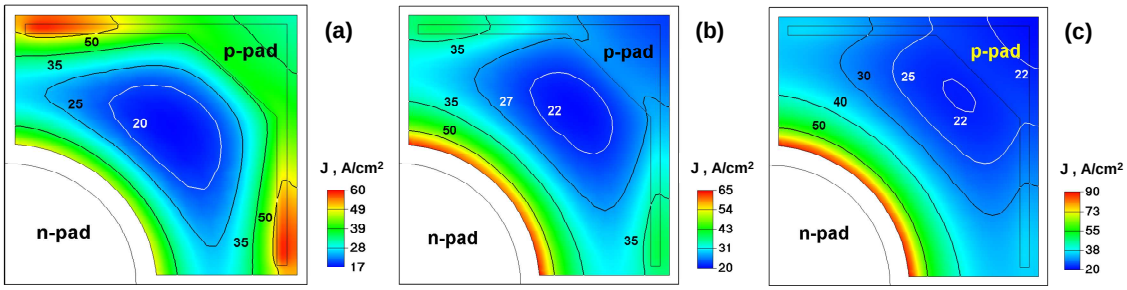

Fig.7 Current density distributions in the active regions of a square-shape LED dice with different thicknesses of ITO spreading layer deposited on the top of *p*-GaN contact layer: (a) 20 nm, (b) 50 nm, and (c) 100 nm [30]. The LED operating current is 20 mA. Markers at isolines correspond to the current density measured in A/cm^2.

One of the approaches to reduce current crowding implies deposition of a current spreading layer made, for example, of transparent conductive indium-tin oxide (ITO) on the top of the *p*-GaN contact layer. The spreading layer forms also a tunnel junction at the *p*-GaN/ITO interface, which can be used instead of the conventional metallic *p*-contact formed to the LED structure. It is commonly believed that such a spreading layer is capable of making more uniform current density distribution in the LED die. Our simulations have, however, revealed quite opposite tendency [30]. In the case of the ITO film with a low lateral conductivity (Fig.7a), the current is localized next to the *p*-electrode edge. Increasing conductivity (Fig.7b) leads to switching of the localization area towards the *n*-electrode edge rather than to homogenization of the current density distribution. The switching is found to depend on the LED operating current, indicating the nonlinear character of the current crowding. Further increase in the lateral conductivity of the ITO film results in ever stronger current localization at the *n*-electrode accompanied by lowering of the LED series resistance.

At the moment, the problem of current crowding is not yet satisfactory solved and the ways for the crowding reduction are still under investigation. Finding such ways is just the task for researchers using LED simulations.

2.4 Light conversion in LED lamps Light conversion in white LED lamps is a comparably novel issue for modeling. The final goals are here: (i) estimation of the LED efficacy and colour quality in the far-field radiation zone in terms of chromatic coordinates, correlated colour temperature (CCT), and colour rendering index (CRI) and (ii) optimization of the conversion medium position inside the lamp, its shape, and phosphor properties to provide uniformity of white light characteristics. An important intermediate step is modeling of light scattering, absorption, and reemission by the phosphor particles disseminated in the conversion medium [31]. Conventional approach to analyze the interaction of light emitted by LED with the phosphor particles is based on the Mie theory capable of predicting the impact of anisotropic light scattering by the particles on the white light characteristics in the far-field zone [32]. The next step

Published in: "Gallium Nitride Materials and Devices VI", Eds. J.-I. Chyi, Y. Nanishi, H. Morkoç, J. Piprek, and E. Yoon, Proc. of SPIE, vol. 7939 (2011) 79391C / **DOI** 10.1117/12.872842

to be made in future is accounting for dispersion of the phosphor particle sizes, as the dispersion control may become an effective way for optimization of light conversion [33].

Up to recently, simulations of light conversion in LEB lamps were primarily focused on their optical design, including remote [34,35] and multiple [35,36] conversion media, omni-directional reflectors [37], and high-reflectivity cups with controlled surface roughness [38]. Investigations into the influence of thermal and electrical conditions of LED operation on the white light characteristics has been started just recently [39,40].

A common problem of the light conversion modeling is the lack of experimental data on such important properties of phosphors, as the internal quantum efficiency and its dependence on temperature, absorption coefficient of the phosphor material and its spectral dispersion, and temperature dependence of the phosphor excitation and emission spectra. To overcome the problem, researchers frequently use special experimental procedures enabling indirect extraction of the lacking information [31,41]. For this, simulations of the corresponding experimental setups and modeling of the LED lamp operation should be coupled with each other.

3 Unsolved problems and future developments

3.1 Overestimated operation voltage and search for extra conductivity channels Practically all the engineering approaches used for modeling III-nitride LEDs are based on a drift-diffusion model of carrier transport in heterostructures. This model has an intrinsic drawback: it predicts remarkably overestimated operation voltage of LEDs with a large number of deep InGaN QWs. The reason for that can be understood from Fig.8a where the band diagram is plotted for an MQW LED structure emitting light at 515 nm. Because of large band offsets at the QW interfaces, every well is surrounded by potential barriers where the electron/hole concentration becomes extremely small, ~10^8-10^9 cm^{-3} and lower, next to the barrier/QW interfaces. A low electrical conductivity of these regions results in a ladder-like conduction and valence band alignment shown in Fig.3a and, eventually, in unrealistically high operation voltage, greater than 5 V at 30 mA (Fig.3c). Besides, the band alignment like that shown in Fig.8a implies a strong ballistic electron leakage to occur in such a structure [42].

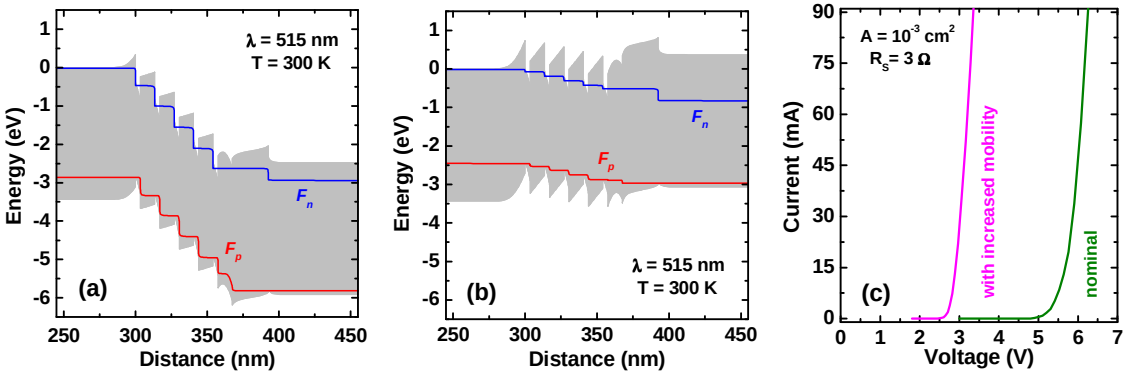

Fig.8 Room temperature band diagrams of an MQW LED structure emitting light at 515 nm computed for the current density of 35 A/cm^2: nominal structure (a) and the structure with the carrier mobilities artificially increased by five orders in magnitude near the tops of barriers surrounding QWs (b); F_n and F_p are the electron and hole quasi-Fermi levels. Current-voltage characteristics of the nominal structure and that with increased mobilities (c) calculated for the active region area $A = 10^{-3}$ cm^2 and LED series resistance $R_s = 3$ Ω.

On the other hand, the operation voltage of less than ~3 V experimentally observed in some green LEDs points out the existence of additional transport mechanisms, apart from those included in the drift-diffusion model, that would provide a higher electrical conductivity in the barriers adjacent to the QWs. Possible candidates for such mechanisms are direct or impurity/defect-assisted carrier tunnelling through the barriers, TD-mediated conductivity, incomplete capture of non-equilibrium carriers in the QWs, and local reduction of the potential barrier heights due to fluctuations of InGaN composition in the QWs. It is not clear at the moment what particular mechanism can be responsible for the enhanced LED structure conductivity. However, if the mobilities of electrons and holes in the barriers are artificially increased to

Published in: "Gallium Nitride Materials and Devices VI", Eds. J.-I. Chyi, Y. Nanishi, H. Morkoç, J. Piprek, and E. Yoon, Proc. of SPIE, vol. 7939 (2011) 79391C / **DOI** 10.1117/12.872842

imitate the still unknown conductivity mechanism and fitted to get a reasonable operation voltage (see Fig.3c), this produces the band alignment in the LED structure (Fig.8b) quite different from that shown in Fig.8a. In particular, the EBL is capable here to suppress completely the electron leakage in the LED *p*-region.

Identification of the basic mechanisms that would provide a sufficiently high electrical conductivity in the MQW barriers, development of the respective physical models for them, and incorporation of the model to the drift-diffusion approach seems to be a challenging task for the nearest future.

3.2 Emission spectra shape, broadening, and blue shift Another problem is related to calculations of the emission spectra from III-nitride LEDs with InGaN QW active regions. Since an ideal QW composition profile and a lorentzian broadening are commonly assumed for the spectrum calculation, the shape of the predicted emission line becomes normally far from that observed experimentally. The predictability can be improved by accounting for the ensemble of localized and delocalized carriers both participating in the light emission [43]. Figure 9a,b plots the emission spectra calculated with the same model of localized electrons and holes, as was used for analysis of IQE in III-nitride QWs (see Sec.2.1). The model predicts the shapes of the emission spectra and their variation with temperature to be in good agreement with observations. However, it also predicts a rather complex behaviour of the spectrum blue shift with the non-equilibrium carrier concentration in the well, depending on the ratio of localization energy U_n+U_p to kT (Fig.9c). So, detailed validation of the model applicability to the spectra calculations is an important issue for future developments.

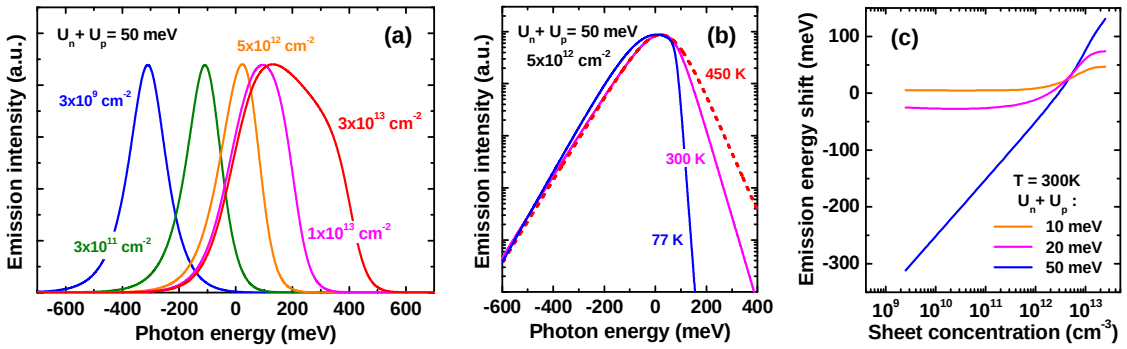

Fig.9 Emission spectra of an InGaN/GaN QW with composition fluctuations at U_n = 35 meV, and U_p = 15 meV: (a) at various sheet concentrations of electrons/holes and room temperature and (b) at different temperatures and sheet carrier concentration of 5×10^{12} cm^{-2} (photon energy is counted from the transition energy in the QW without compositional fluctuations). Blue shift of the peak photon energy as a function of carrier concentrations (c).

The extension of the localized states model to predicting the optical characteristics of InGaN QWs is expected to have some other consequences. First, the carrier recombination rate may now depend on the electron and hole concentrations and temperature in a manner different from the conventional one due to modified carrier density of states in the QW. Second, additional spectrum broadening related to the carrier localization should affect the optical gain in laser diode heterostructures. All these aspects require a careful examination by comparison with available observations.

3.3 Cavity effects Strong modulation of LED external quantum efficiency upon increasing thickness of the *p*-GaN contact layer separating the active region and highly reflective metallic *p*-electrode has been demonstrated experimentally [44]. The effect originates from self-interference of the emitted photon caused by its reflection from the electrode and has a dual manifestation. First, the probability of light emission goes up due to increasing magnitude of the photon electromagnetic field in the LED active region. Second, the interference results in an angular modulation of the emission pattern from the active region, affecting overall LEE [44]. Consistent model of this cavity effect is not yet developed despite its importance for correct predicting of the device characteristics.

3.4 General factors affecting predictability of LED simulations Except for the model improvement required for more adequate LED simulations, there are other factors affecting the model predictability.

Published in: "Gallium Nitride Materials and Devices VI", Eds. J.-I. Chyi, Y. Nanishi, H. Morkoç, J. Piprek, and E. Yoon, Proc. of SPIE, vol. 7939 (2011) 79391C / **DOI** 10.1117/12.872842

First of all, some important materials properties of III-nitride compounds, like conduction and valence band offsets, spontaneous electric polarization, deformation potentials, ionization energies of donors and acceptors, hole effective masses, Auger recombination coefficients, etc., are still known with insufficient accuracy. In addition, the necessity of using advanced physical models requires knowing additional parameters related, for instance, to TDs or localized electron/hole states. The properties of accompanying materials used for LED fabrication also need a careful evaluation. For example, the optical properties of metals used as electrodes have a strong dispersion in the visible and UV spectral ranges, which should be accurately considered to predict properly LEE from an LED die. Another example is ITO having interrelated electrical and optical properties. Making simulations, one should specify the electrical conductivity of the ITO film, as well as the electron mobility, in order to estimate the materials optical characteristics depending on both parameters [30].

Not only the reliable materials properties but also some additional information on the LED structure is frequently needed for accurate simulations. First, the LED band structure is quite sensitive to distribution of polarization charges depending on particular composition profile and strain. Because of indium surface segregation, the InGaN QW profile may by much different from the nominal one, providing considerable broadening and smoothing of the QW interfaces and penetration of indium in the QW barriers [45,46]. Second, the strain in the well may depend on both the composition profile and stress relaxation occurring in the layers preceding the QW. And, considerable Mg redistribution next to the active region during growth of various LED structures has been reported, eventually affecting the emission efficiency [47,48]. All the above effects are crucial for LED operation and can be allowed for in simulation on the basis of additional experimental information or advanced theoretical studies.

4 Conclusion As discussed above, there is still a big room for improvement of the existing physical models and building up new models accounting for specific properties of III-nitride materials and devices. In addition, much effort should be made to understand better effects of III-nitride compound microstructure on the carrier transport and recombination processes. Such developments are expected to form the main stream in the future research. However, this will not provide any guideline for understanding the impact of technological factors and, first of all, of heterostructure growth conditions on the operation and characteristics of III-nitride LEDs, despite its evident importance. On the other hand, it is hard to expect a rapid progress in experimental studies of such issues, as strain relaxation and impurity redistribution in LED structures during growth, modification of the QW composition profile and instability of the QW thickness caused by indium surface segregation, as well as other technological factors. In this respect, coupled modeling of heterostructure growth and device operation would be a solution to this problem. The analysis of indium incorporation during epitaxial growth and optical transitions in strained InGaN/GaN materials and QWs [49] provides an example of a small first step forward in this direction. Alternatively, detailed experimental information has to be invoked to highlight the contribution of technological factors to formation of the composition, doping, and defect density profiles in LED heterostructures.

Acknowledgment: I am grateful to my colleagues, I. Yu. Evstratov, K. A. Bulashevich, V. F. Mymrin, M. S. Ramm, M. V. Bogdanov, and A. I. Zhmakin, contributed much to development, numerical implementation, and validation of models for III-nitride LED simulation.

References

[1] Nakamura, S., Mukai, T. and Senoh, M., "Candela-class high-brightness InGaN/AlGaN double-heterostructure blue-light-emitting diodes", Appl. Phys. Lett. 64(13), 1687-1689 (1994).

[2] Nakamura, S., Senoh, M., Iwasa, N. and Nagahama, S.-I., "High-power InGaN single-quantum-well-structure blue and violet light-emitting diodes", Appl. Phys. Lett. 67(13), 1868-1871 (1995).

[3] Krames, M. R., Shchekin, O. B., Mueler-Mach, R., Mueler, G. O., Zhou, L., Harbers, G. and Craford, M. G., "Status and Future of High-Power Light-Emitting Diodes for Solid-State Lighting", J. Display Technol., 3(2), 160-175 (2007).

[4] Härle, V., Hahn, B., Kaiser, S., Weimar, A., Eisert, D., Bader, S., Plössl, A. and Eberhard, F., "Light extraction technologies for high-efficiency GaInN-LED devices", Proc. SPIE 4996, 133-137 (2003).

[5] Shchekin, O. B., Epler, J. E., Trottier, T. A., Margalith, T., Steigerwald, D. A., Holcomb, M. O., Martin, P. S. and Krames, M. R., "High performance thin-film flip-chip InGaN–GaN light-emitting diodes", Appl. Phys. Lett. 89(7), 071109 (2006).

[6] Chichibu, S. F., Marchand, H., Minsky, M. S., Keller, S., Fini, P. T., Ibbetson, J. P., Fleischer, S. B., Speck, J. S. J., Bowers, E., Hu, E., Mishra, U. K., DenBaars, S. P., Deguchi, T., Sota, T. and Nakamura, S., "Emission mechanisms of bulk GaN and InGaN quantum wells prepared by lateral epitaxial overgrowth", Appl. Phys. Lett. 74(10), 1460-1462 (1999).
[7] Bernardini, F., Fiorentini, V. and Vanderbilt, D., "Spontaneous polarization and piezoelectric constants of III-V nitrides", Phys. Rev. B 56(16), R10024-R10027 (1997).
[8] Bernardini, F., Fiorentini, V. and Vanderbilt, D., "Accurate calculation of polarization-related quantities in semiconductors", Phys. Rev. B 63(19), 193201 (2001).
[9] Bernardini, F. and Fiorentini, V., "Nonlinear macroscopic polarization in III-V nitride alloys", Phys. Rev. B 64(8), 085207 (2001).
[10] Davydov, V. Yu., Klochikhin, A. A., Emtsev, V. V., Kurdyukov, D. A., Ivanov, S. V., Vekshin,V. A., Bechstedt, F., Furthmüller, J., Aderhold, J., Graul, J., Mudryi, A. V., Harima, H., Hashomoto, A., Yamamoto, A. and Haller, E. E., "Band Gap of Hexagonal InN and InGaN Alloys", Phys. Stat. Solidi (b), 234(3), 787-795 (2002).
[11] Bulashevich, K. A. and Karpov, S. Yu., "Is Auger recombination responsible for the efficiency rollover in III-nitride light-emitting diodes?", Phys. Stat. Solidi (c), 5(6), 2066-2069 (2008).
[12] Shen, Y. C., Mueler, G. O., Watanabe, S., Gardner, N. F., Munkholm, A. and Krames, M. R., "Auger recombination in InGaN measured by photoluminescence", Appl. Phys. Lett. 91(14), 141101 (2007).
[13] Piprek, J., Katona, T., DenBaars, S. P. and Li, S., "3D Simulation and Analysis of AlGaN/GaN Ultraviolet Light Emitting Diodes", Proc. SPIE 5366, 127-136 (2004).
[14] Karpov, S. Yu., Bulashevich, K. A., Zhmakin, I. A., Nestoklon, M. O., Mymrin, V. F. and Makarov, Yu. N., "Carrier injection and light emission in visible and UV nitride LEDs by modeling", Phys. Stat. Solidi (c), 241(12), 2668-2671 (2004).
[15] Piprek, J. and Nakamura, S., "Physics of High-Power InGaN/GaN Lasers", IEE Proc. Optoelectronics 149(4), 145-151 (2002).
[16] Karpov, S. Yu. and Makarov, Yu. N., "Dislocation Effect on Light Emission Efficiency in Gallium Nitride", Appl. Phys. Lett. 81(23), 4721-4723 (2002).
[17] Piprek, J., "Efficiency droop in nitride-based light-emitting diodes", Phys. Stat. Solidi (a), 207(10), 2217-2225 (2010).
[18] Delaney, K. T., Rinke, P., and Van de Walle, C. G., "Auger recombination rates in nitrides from first principles", Appl. Phys. Lett. 94, 191109 (2009).
[19] Chernyakov, A. E., Sobolev, M. M., Ratnikov, V. V., Shmidt, N. M. and Yakimov, E. B., "Nonradiative recombination dynamics in InGaN/GaN LED defect system", Superlattices and Microstructures, 45(4/5), 301-307 (2009).
[20] Laubsch, A., Sabathil, M., Bergbauer, W., Strassburg, M., Lugauer, H., Peter, M., Lutgen, S., Linder, N., Streubel, K., Hader, J., Moloney, J. V., Pasenow, B. and Koch, S. W., "On the origin of IQE 'droop' in InGaN LEDs", Phys. Stat. Solidi (c), 6(S2), S913–S916 (2009).
[21] Karpov, S. Yu., "Effect of localized states on internal quantum efficiency of III-nitride LEDs", Phys. Stat. Solidi RRL, 4(11), 320-322 (2010.
[22] Karpov, S. Yu., Bulashevich, K. A., Zhmakin, I. A., Nestoklon, M. O., Mymrin, V. F. and Makarov, Yu. N., "Carrier injection and light emission in visible and UV nitride LEDs by modeling", Phys. Stat. Solidi (b), 241(12), 2668-2671 (2004).
[23] Jena, D., Heikman, S., Green, D., Buttari, D., Coffie, R., Xing, H., Keller, S., DenBaars, S., Speck, J. S. and Mishra, U. K., "Realization of wide electron slabs by polarization bulk doping in graded III–V nitride semiconductor alloys", Appl. Phys. Lett. 81(23), 4395-4397 (2002).
[24] Bulashevich, K. A., Mymrin, V. F. and Karpov, S. Yu., "Control of electron leakage in III-nitride laser diodes by blocking layer design, using distributed polarization doping", Proc. 3rd Asia-Pacific Workshop on Widegap Semiconductors, 192-1944 (2007).
[25] Simon, J., Protasenko, V., Lian, C., Xing, H. and Jena, D., "Polarization-Induced Hole Doping in Wide-Band-Gap Uniaxial Semiconductor Heterostructures", Science, 327(5961), 60-64 (2010).
[26] Bulashevich, K. A., Evstratov, I. Yu., Mymrin, V. F. and Karpov, S. Yu., "Current spreading and thermal effects in blue LED dice", Phys. Stat. Solidi (c) 4(1), 45-48 (2007).
[27] López, T. and Margalith, T., "Electro-Thermal Modelling of High Power Light Emitting Diodes Based on Experimental Device Characterisation", Proc. Comsol Conference 2008, Boston MA, October 9-11 (2008).
[28] Bogdanov, M. V., Bulashevich, K. A., Khokhlev, O. V., Evstratov, I. Yu., Ramm, M. S. and Karpov, S. Yu., "Current crowding effect on light extraction efficiency of thin-film LEDs", Phys. Stat. Solidi (c), 7(7/8), 2124-2126 (2010).
[29] http://www.str-soft.com/products/SimuLED/

[30] Bogdanov, M. V., Bulashevich, K. A., Khokhlev, O. V., Evstratov, I. Yu., Ramm, M. S. and Karpov, S. Yu., "Effect of ITO spreading layer on performance of blue light-emitting diodes", Phys. Stat. Solidi (c), 7(7/8), 2127-2129 (2010).

[31] Linder, N., Eisert, D., Jermann, F. and Berben, D., "Simulation of LEDs with Phosphorescent Media for the Generation of White Light", in: Ed. Piprek, J., [Nitride Semiconductor Device: Principles and Simulation], WILEY-VCH Verlag GmbH & Co. KGaA, Weinheim, 327-351 (2007).

[32] Sommer, C., Wenzl, F.-P., Hartmann, P., Pachler, P., Schweighart, M., Tasch, S. and Leising, G., "Tailoring of the Color Conversion Elements in Phosphor-Converted High-Power LEDs by Optical Simulations", IEEE Photon. Technol. Lett., 20(9), 739-741 (2008).

[33] Sommer, C., Krenn, J. R., Hartmann, P., Pachler, P., Schweighart, M., Tasch, S. and Wenzl, F.-P., "The Effect of the Phosphor Particle Sizes on the Angular Homogeneity of Phosphor-Converted High-Power White LED Light Sources", IEEE J. Selected Topics in Quantum Electronics, 15(4), 1181-1188 (2009).

[34] Zhu, Y. and Narendran, N., "Optimizing the Performance of Remote Phosphor LEDs", J. Light & Vis. Env. 32(2), 115-119 (2008).

[35] Zhu, Y. and Narendran, N., "Investigation of Remote-Phosphor White Light-Emitting Diodes with Multi-Phosphor Layers", Jpn. J. Appl. Phys. 49(10), 100203 (2010).

[36] Won, Y.-H., Jang, H. S., Cho, K. W., Song, Y. S., Jeon, D. Y. and Kwon, H. K., "Effect of phosphor geometry on the luminous efficiency of high-power white light-emitting diodes with excellent color rendering property", Optics Lett. 34(1), 1-3 (2009).

[37] Chen S.-W., Su J.-C., Lu C.-L., Song S.-F. and Chen, J.-H., "Phosphors-conversion white light LED with omni-directional reflector", Proc. SPIE 7138, 71382D (2008).

[38] Xi, Y. Li, X., Kim, J. K., Mont, F., Gessmann, Th., Luo, H. and Schubert, E. F., "Quantitative assessment of diffusivity and specularity of surface-textured reflectors for light extraction in light-emitting diodes", J. Vac. Sci. Technol. A 24(4), 1627-1630 (2006).

[39] Fan, B., Wu, H., Zhao, Y., Xian, Y. and Wang, G., "Study of Phosphor Thermal-Isolated Packaging Technologies for High-Power White Light-Emitting Diodes", IEEE Photon. Technol. Lett. 19(15), 1121-1123 (2007).

[40] Khokhlev, O. V., Bord, O. V., Bogdanov, M. V., Bulashevich, K. A., Ramm, M. S., Evstratov I. Yu. and Karpov, S. Yu., "Effect of Temperature and Current Variation on the Color Quality of White Light-Emitting Diodes", Proc. 12th Int. Symp. On the Science and Technology of Light Sources & 3rd Int. Conf. on White LEDs and Solid State Lighting, FAST-LS Ltd., Sheffield, 29-30 (2010).

[41] Sun, C.-C., Chen, C.-Y, He, H.-Y, Chen, C.-C., Chien, W.-T., Lee, T.-X. and Yang, T.-H., "Precise optical modeling for silicate-based white LEDs", Optics Express 16(24), 20060-20066 (2008).

[42] Kisin, M. V. and El-Ghoroury, H. S., "Injection characteristics of polar and nonpolar multiple-QW structures and active region ballistic overshoot", accepted in Phys. Stat. Solidi (c)

[43] Jacobson, M. A., Nelson, D. K., Konstantinov, O. V. and Matveentsev, A. V., "The tail of localized states in the band gap of the quantum well in the $In_{0.2}Ga_{0.8}N/GaN$ system and its effect on the laser-excited photoluminescence spectrum", Semiconductors, 39(12), 1410-1414 (2005).

[44] Shen, Y. C., Wierer, J. J., Krames, M. R., Ludowise, M. J., Misra, M. S., Ahmed, F., Kim, A. Y., Mueller, G. O., Bhat, J. C., Stockman, S. A. and P. S. Martin, "Optical cavity effects in InGaN/GaN quantum-well-heterostructure flip-chip light-emitting diodes", Appl. Phys. Lett. 82(14), 2221-2223 (2003).

[45] Kisielowski, C., Liliental-Weber, Z. and Nakamura, S., "Atomic Scale Indium Distribution in a $GaN/In_{0.43}Ga_{0.57}N/Al_{0.1}Ga_{0.9}N$ Quantum Well Structure", Jpn. J. Appl. Phys. Pt.1, 36(11), 6932-6936 (1997).

[46] Talalaev, R. A., (a), Karpov, S. Yu., Evstratov, I. Yu. and Makarov, Yu. N., "Indium Segregation in MOVPE Grown InGaN-Based Heterostructures", Phys. Stat. Solidi (c) 0(1), 311-314 (2002).

[47] Köhler, K., Stephan, T., Perona, A., Wiegert, J., Maier, M., Kunzer, M. and Wagner, J., "Control of the Mg doping profile in III-N light-emitting diodes and its effect on the electroluminescence efficiency", J. Appl. Phys. 97(10), 104914 (2005).

[48] Köhler, K., Perona, A., Maier, M., Wiegert, J., Kunzer, M. and Wagner, J., "Mg doping profile in III–N light emitting diodes in close proximity to the active region", Phys. Stat. Solidi (a) 203(7),1802-1805 (2006).

[49] Durnev, M. V., Omelchenko, A. V., Yakovlev, E. V., Evstratov, I. Yu. and Karpov, S. Yu., "Indium incorporation and optical transitions in InGaN bulk materials and quantum wells with arbitrary polarity", Appl. Phys. Lett. 97(5), 051904 (2010).